Phasor-Based Secondary Arc Extinction Detection Method for Shunt Compensated Transmission Lines

Karcius M. C. Dantas, Matheus Alves, Felipe V. Lopes, Flavio B. Costa, Kleber M. Silva

***Abstract*—Secondary arc extinction detection (SAED) is essential for adaptive single-phase auto-reclosing (ASPAR) success. Many SAED/ASPAR methods have been proposed in the literature. However, most of them do not present a practical approach for field implementation. A new methodology is proposed aiming to provide an effective and practical phasor-based SAED/ASPAR scheme for shunt compensated transmission lines. That scheme consists in analyzing the line side voltage phasors in the modal domain to safely and rapidly identify the secondary arc extinction, requiring only the voltage phasors at one line terminal. Furthermore, it can be easily implemented in readily available IED (Intelligent Electronic Devices), such that no additional hardware or equipment is required, being quite suitable for real-world applications. Therefore, a new mathematical formulation is developed considering the shunt and neutral reactors effects. Then, the SAED/ASPAR applicability and limitations for shunt compensated lines are clearly defined. Data from the Brazilian Power Grid and field oscillographic recordings are used for case studies. The results attest the efficiency and reliability of the proposed methodology.**

***Keywords*—Phasor Measurements; Secondary Arc Extinction; Single-Phase Auto-reclosing; Transmission Lines.**

I. Introduction

FAULTS on power systems may cause energy supply interruption and degrade the efficiency and quality of services provided by the utilities. Thus, protecting the power system and providing its prompt restoration after a fault occurrence are main concerns to maintain the continuous and economical supply of electricity. Among all system equipment, transmission lines (TL) are mostly susceptible to faults mainly because of their extension and environmental exposure. In Brazil, for example, there are more than 175.000 kilometers of lines rated 230 kV and above. Besides, more than 80% of line faults are single-phase-to-ground and most of them are self extinguished [1], [2]. That is why Single-Phase Auto-Reclosing (SPAR) of lines stands out for decades [3]–[6]. At first, SPAR was proposed to open the TL faulted phase and reclose it after a fixed dead time [7], [8]. However, an unsuccessful reclosing could occur in the case of a permanent fault. Then, aiming to avoid reclosing onto fault, Secondary Arc Extinction Detection (SAED) methods have been proposed and the term Adaptive Single-Phase Auto-Reclosing (ASPAR) arose due to the possibility of adapting the line dead time [9], [10]. Afterwards, many SAED/ASPAR approaches have been proposed in the literature for non-compensated or shunt compensated transmission lines (SCTL). Those methods are based on phasor analysis, harmonic signature, artificial neural networks, wavelet transform, support vector machine, etc [11]–[26]. However, most of them do not present a practical approach for field implementation, what may limit their application.

In [27], the authors presented a practical approach to leverage existing relays structure aiming to improve SPAR applications. A simple and effective phasor-based single-phase auto-reclosing scheme for non-compensated TL was proposed and embedded in a commercially available relay equipped with a free-form programming logic. That scheme consists on analyzing the line side voltage phasors in the modal domain to safely and rapidly identify the secondary arc extinction, requiring only the voltage phasors at one line terminal [28]. Additionally, it has a very low computational burden, is much simpler than most existing SPAR techniques, can be easily implemented in readily available IED (Intelligent Electronic Devices), such that no additional hardware or equipment is required, and presents a better performance on SAED beeing much faster than existing phasor-based SPAR methods and even faster than sophisticated or higher burden SPAR methods. However, although the results attested the effectiveness of that SAED/ASPAR method, as well as the feasibility of the proposed practical approach for real-world prompt use, its application for SCTL was still not fully addressed.

In this paper, the phasor-based secondary arc extinction detection approach presented in [28] is addressed for single-phase auto-reclosing of SCTL. A new mathematical method is developed considering the shunt and the neutral reactors effects. Therefore, the approach applicability and limitations for shunt compensated TL are clearly defined. As a consequence of using the proposed formulation, now it is possible to safely determine if that approach is suitable or not for any homogeneous transmission line. Data from the Brazilian Power Grid were used for the case studies, including field oscillographic records. The results prove the developed mathematical formulation effectiveness and attest the reliability of the presented analysis.

This work was supported in part by the Brazil's National Council for Scientific and Technological Development (CNPq). K. M. C. Dantas is with the Department of Electrical Engineering, Federal University of Campina Grande - UFCG, Brazil (e-mail of corresponding author: karcius@dee.ufcg.edu.br). M. Alves is a post-graduate student at the Department of Electrical Engineering, Federal University of Campina Grande - UFCG, Campina Grande - Brazil (e-mail: matheus.rocha.alves@ee.ufcg.edu.br). F. V. Lopes is with the Department of Electrical Engineering, Federal University of Paraíba - UFPB, João Pessoa - Brazil (e-mail: felipelopes@cear.ufpb.br). F. B. Costa is with the Department of Electrical Engineering and Computer, Michigan Technological University - MTU, Houghton - USA (e-mail: fbcosta@mtu.edu). K. M. Silva is with the Department of Electrical Engineering, University of Brasília - UnB, Brasília - Brazil (e-mail: klebermelo@unb.br).

Paper submitted to the International Conference on Power Systems Transients (IPST2025) in Guadalajara, Mexico, June 8-12, 2025.

II. Existing Phasor-Based SPAR Scheme for Non-compensated Lines

The basics on the phasor-based single-phase auto-reclosing scheme proposed in [28] for non-compensated transmission lines is presented in this section for better understanding. In that approach, aiming to determine the secondary arc extinction time, the Clarke's matrix is applied to the line side voltage rms phasors ($\hat{V}_A, \hat{V}_B$ and $\hat{V}_C$), yielding the modal phasors ($\hat{V}_0$ and $\hat{V}_\alpha$):

$$\hat{V}_0 = \frac{1}{3}\left(\hat{V}_A + \hat{V}_B + \hat{V}_C\right) \tag{1}$$

and

$$\hat{V}_\alpha = \frac{1}{3}\left(2\hat{V}_A - \hat{V}_B - \hat{V}_C\right) \ . \tag{2}$$

After the single-phase opening due to a single-line-to-ground fault at phase A, ideally $\left|\hat{V}_A\right| << \left|\hat{V}_B + \hat{V}_C\right|$. In this situation, while the fault persists in the line, it can be shown that:

$$\frac{\hat{V}_0}{-\hat{V}_\alpha} \approx 1 \ . \tag{3}$$

After the secondary arc extinction, the phase-to-ground voltage at the opened line phase recovers and its value can be approximated by:

$$\hat{V}_A = K\left(\hat{V}_B + \hat{V}_C\right) \tag{4}$$

where

$$K = \frac{C_m}{C_s + 2C_m} \tag{5}$$

for a non-compensated line. C_m is the capacitance between the line phases and C_s is the capacitance between each phase and the earth. Substituting (4) in (1) and (2), the following equality is valid after the fault extinction:

$$\frac{\hat{V}_0}{-\hat{V}_\alpha} = \frac{1+K}{1-2K} \ . \tag{6}$$

The absolute value for the ratio $\frac{\hat{V}_0}{-\hat{V}_\alpha}$ is given by:

$$R = \left|\frac{\hat{V}_0}{-\hat{V}_\alpha}\right| \ . \tag{7}$$

which will always be greater than 1 after the fault extinction, because $0 < K < 0.5$, according to (5).

In this way, (7) can be used for secondary arc extinction detection: according to (3) and (6), if R is close to one, then the fault persists on the line; conversely, if R is greater than one, then the fault has been extincted. However, these statements are valid for the ideal situation where $\left|\hat{V}_A\right| << \left|\hat{V}_B + \hat{V}_C\right|$. Then, instead of comparing R to 1, R is compared to a threshold λ that safely indicate the presence of the fault. A thorough analysis of different 230 and 500 kV transmission lines from the Brazilian Power Grid was carried out in [28] to define a proper value for λ. Then, a value of 1.28 was proposed, which is used here.

III. Proposed Methodology

The practical approach for SAED/ASPAR, described in Section II, was developed for non-compensated lines. Therefore, a new mathematical development is presented in this section aiming to safely extend the application of that approach for shunt compensated lines. For this purpose, (5), and consequently (7), are reevaluated to include the shunt and neutral reactors effects.

A. Transmission Lines and Shunt Reactors Considerations

In the following, the theoretical considerations for transmission lines and shunt reactors are presented for the proposed mathematical development. Fig. 1 shows the line phases (A, B and C) and the respective C_s and C_m capacitances. Thus, the line positive sequence capacitance can be defined as:

$$C_1 = C_s + 3C_m \ . \tag{8}$$

$\hat{I}_A$, $\hat{I}_B$ and $\hat{I}_C$ are the electrical current phasors injected at each phase of the line terminal.

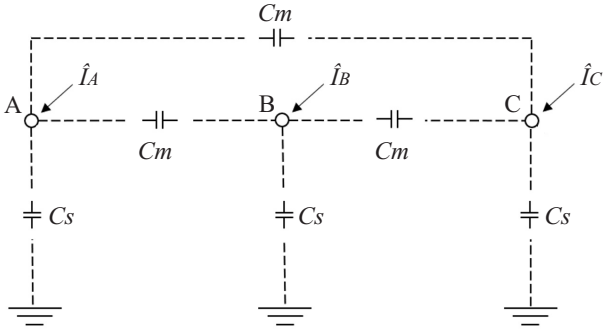

Fig. 1. Transmission line capacitances representation.

Fig. 2 shows a typical four-legged shunt-reactor (on the left-side hand), and the equivalent circuit (on the right-side hand), which emphasizes the equivalent inductances L_s and L_m for the reactor. L is the phase inductance and L_n is the neutral inductance for the four-legged shunt-reactor. The terminals for each phase of this equipment are indicated by A, B and C.

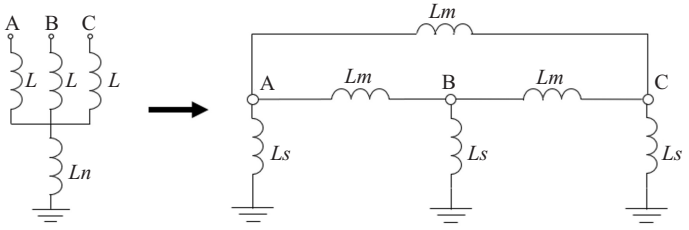

Fig. 2. Shunt reactor inductances representation.

Yet, from Fig. 2:

$$L_s = L + 3L_n \tag{9}$$

and

$$L_m = \frac{L(L+3L_n)}{L_n} \ . \tag{10}$$

Let $L_0 = L + 3L_n$ and $L_1 = L$ be the zero and positive sequence inductances for the shunt reactor, respectively. Then, define

$$\rho = \frac{L_0}{L_1} \ = \frac{L+3L_n}{L} \ . \tag{11}$$

Rewriting (11) in terms of L_n:

$$L_n = \left(\frac{\rho-1}{3}\right) L \rightarrow L_n = \varphi L \ , \tag{12}$$

where $\varphi = \left(\frac{\rho-1}{3}\right)$.

Finally, let g be the line compensation degree provided by the shunt reactor, defined as:

$$g = \frac{1}{\omega^2 L_1 C_1} \ . \tag{13}$$

B. Mathematical Development

Considering that the shunt reactor shown in Fig. 2 is connected to the transmission line phases shown in Fig. 1, by using nodal analysis yields:

$$\begin{bmatrix} \hat{I}_A \\ \hat{I}_B \\ \hat{I}_C \end{bmatrix} = \begin{bmatrix} Y_s & -Y_m & -Y_m \\ -Y_m & Y_s & -Y_m \\ -Y_m & -Y_m & Y_s \end{bmatrix} \begin{bmatrix} \hat{V}_A \\ \hat{V}_B \\ \hat{V}_C \end{bmatrix} \ , \tag{14}$$

where

$$Y_s = j\omega \left(C_s + 2C_m - \frac{1}{\omega^2 L_s} - \frac{2}{\omega^2 L_m} \right) \tag{15}$$

and

$$Y_m = j\omega \left(C_m - \frac{1}{\omega^2 L_m} \right) \ . \tag{16}$$

For a single-phase-to-ground fault at phase A, after the single-phase opening, it can be stated that $\hat{I}_A = 0$. Then, from the first line of (14):

$$\hat{V}_A = K' \left(\hat{V}_B + \hat{V}_C \right) \ , \tag{17}$$

where

$$K' = \frac{Y_m}{Y_s} \ . \tag{18}$$

Substituting (9), (10), (15), and (16) in (18):

$$K' = \left[\frac{C_m - \dfrac{L_n}{\omega^2 L\,(L+3L_n)}}{C_s + 2C_m - \dfrac{1}{\omega^2\,(L+3L_n)} - \dfrac{2L_n}{\omega^2\,(L+3L_n)}} \right] . \tag{19}$$

Then, substituting (12) and (13) in (19):

$$K' = \left[\frac{C_m - \dfrac{g\varphi C_1}{(1+3\varphi)}}{C_s + 2C_m - \dfrac{gC_1}{(1+3\varphi)} - \dfrac{2\varphi g C_1}{(1+3\varphi)}} \right] . \tag{20}$$

Finally, considering (8) and (11), and after few mathematical manipulations, it results in:

$$K' = \frac{3C_m\left[\rho + g(1-\rho)\right] - C_s g(\rho-1)}{3\left[\rho(C_s+2C_m) - g(C_s+3C_m)\right] - 2g(\rho-1)(C_s+3C_m)} \ . \tag{21}$$

By using (17) and (21) it is possible to correlate the faulty phase voltage with the healthy phase voltages taking into account the shunt and the neutral reactors effects. Additionally, (21) can also be applied for non-compensated lines by considering $g = 0$ and $\rho = 1$. Thus, a new parameter for secondary arc extinction detection is derived for both non-compensated and shunt compensated lines:

$$R' = \left| \frac{1+K'}{1-2K'} \right| \ . \tag{22}$$

It is noteworthy that $\left(\frac{1+K'}{1-2K'}\right)$ may assume positive or negative values, depending on K'. Therefore, its absolute value is used to detect the arc extinction by comparing it to λ.

C. Mathematical and Parametric Analysis for K' and R'

According to (5), K may theoretically vary from 0 to 0.5 for non-compensated lines, implying that R, defined in (7), will always be greater than 1 after the secondary arc extinction. The statistical study carried out in [28] shows that it is safe to consider that the arc is extinguished when $R > 1.28$. However, this condition has not been observed for all shunt compensated lines. For such cases, the range for K' and R', defined in (21) and (22), respectively, cannot be trivially set. This is due to the complex relation between K' and the parameters of the lines and the shunt reactors (C_s, C_m, g and ρ). Then, mathematical and parametric analysis are essential for better understanding K' and R' for SCTL.

Here, the behavior of K', and consequently R', is addressed. Data from different 230 and 500 kV SCTL from the Brazilian Power Grid were used for the analysis, as shown in Table I. Where $R_{0/1}$, $X_{0/1}$ and $B_{0/1}$ accounts for the zero and positive sequence series resistance, series reactance, and shunt susceptance of the line, respectively. Representative scenarios were considered, including double-circuit lines (e.g. Lines I to VII and XI to XX) and both series and shunt compensated lines (e.g. Lines VII, IX, XI, XV, XVII and XX). Additionally, actual atypical scenarios which are generally designed due to specific technical requirements were evaluated, including a relatively short line with a high shunt compensation level (e.g. Line III, which is part of a longer sectionalized line) and a long line with a low shunt compensation level (e.g. Line XII, which is both series and shunt compensated).

Regarding the shunt reactors parameters, it is well known that g is usually set to meet the voltage requirements for the power system, especially due to the Ferranti effect, while ρ is set to attend secondary arc current requirements. Figs. 3, 4 and 5 are presented below with the aim of outlining how K' and R' behave with respect to different line parameters and a wide range of values for g and ρ.

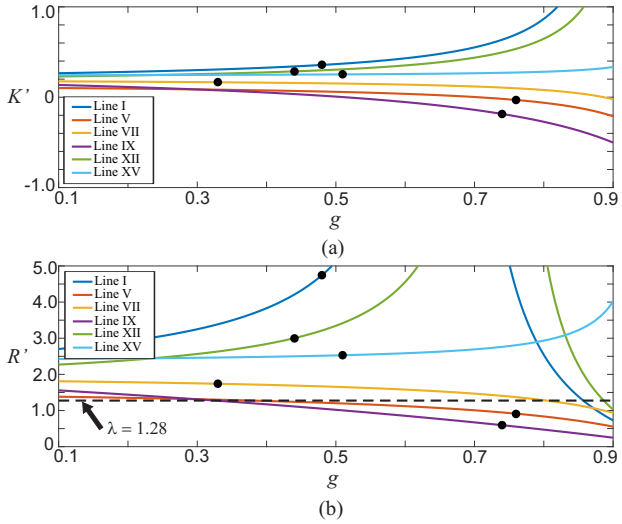

Fig. 3. Behavior of K' and R' for different shunt compensated lines as a function of the compensation degree g. (a) K'. (b) R'.

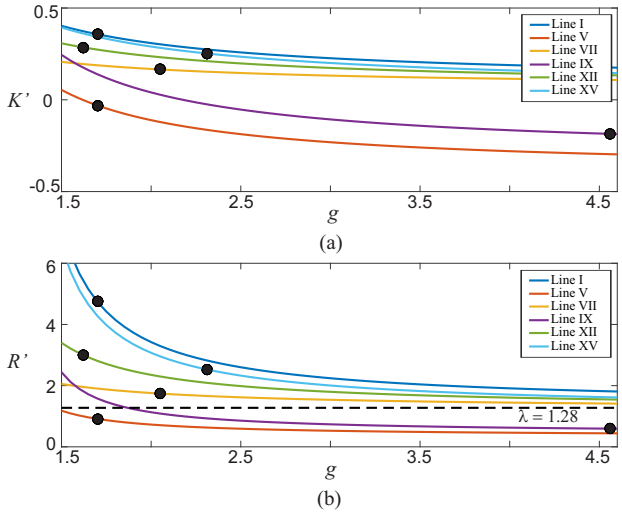

Fig. 4. Behavior of K' and R' for different shunt compensated lines as a function of ρ. (a) K'. (b) R'.

Fig. 3 shows the behavior of K' and R' for some of the lines parameters presented in Table I as a function of the compensation degree g. In that figure, C_s, C_m and ρ are kept constant to compute K' and R' for each line, while g varies from 10% to 90% just for better understanding. The dark dots indicate the exactly K' and R' values for g indicated in Table I for each line. According to Fig. 3(a), K' may vary in different ranges, in agreement with the line parameters and compensation degree, and can assume both positive and

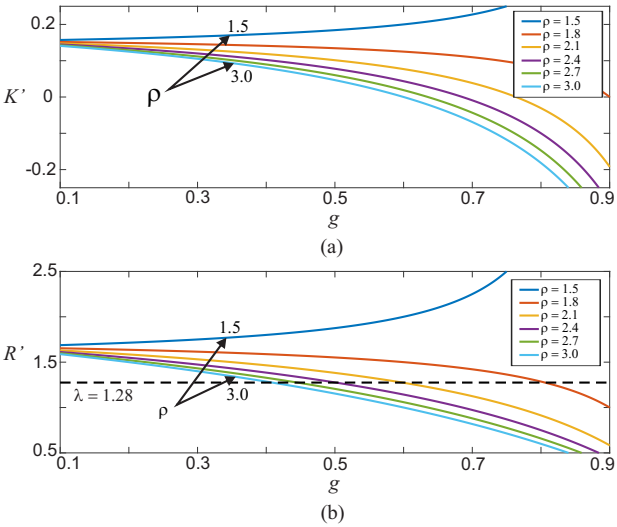

Fig. 5. Behavior of K' and R' for Line IX, considering different ρ. (a) K'. (b) R'.

negative values. For $g = 80\%$, e.g., K' varies from -0.27 to 0.87, directly influencing R', which in turn varies from 0.47 to 10.25. Additionally, by observing Fig. 3(b), it is noteworthy to point out that for some cases (Line XV, for example) R' will always be greater than the threshold $\lambda = 1.28$, regardless of g, indicating that the approach presented in [28] for SAED/ASPAR can be applied for that line with no constraints. Conversely, in the case of Line IX, e.g., that approach cannot be applied for the typical practical values of $g > 30\%$, since $R' < \lambda$ for that range. Thus, by analyzing the dark dots on Fig. 3(b), which represents the exactly data provided in Table I, it can be concluded that the approach presented in [28] for SAED/ASPAR can be fully applied to Lines I, VII, XII and XV, while it cannot be applied to Lines V and IX.

Fig. 4 shows the behavior of K' and R' as a function of the shunt reactor sequence inductances ratio ρ, for the same lines analyzed in Fig. 3. Now, C_s, C_m and g are kept constant to compute K' and R' for each line, while ρ varies from 1.5 to 4.6. Just like before, the dark dots indicate the exactly K' and R' values for ρ indicated in Table I for each line. According to Fig. 4(a), K' may vary in different ranges, in agreement with ρ. For $\rho = 1.8$, e.g., K' varies from -0.13 to 0.30, directly influencing R', which in turn varies from 0.69 to 3.18. It can be seen in Fig. 4(b) that, regardless of ρ, R' will always be greater than the threshold λ for Lines I, VII, XII and XV. Which indicates that the proposed SAED/SPAR can be fully applied to those lines. On the other hand, R' will always be smaller than λ for Line V, indicated that the method cannot be applied for that line. Finally, for Line IX, it can be observed that $R' < \lambda$ only when $\rho > 1.87$. Then, aiming for further clarification on the behavior of K' and R' for this line, Fig. 5 is presented. It can be observed in that figure that the higher the ρ, the lower the K', which also implies in lower R'. For a 55% shunt compensation degree, e.g., the SAED/SPAR method could be applied for ρ up to 2.1. However, it could not be applied for $\rho = 2.4$ and above.

TABLE I
TRANSMISSION LINES AND SHUNT COMPENSATION DATA FROM THE BRAZILIAN POWER GRID.

Voltage	Line	Length [km]	R_1 [Ω/km]	X_1 [Ω/km]	B_1 [μS/km]	R_0 [Ω/km]	X_0 [Ω/km]	B_0 [μS/km]	g [%]	ρ
230 kV	I[1]	150.0	0.043	0.319	5.259	0.749	2.585	2.061	48	1.70
	II[1]	165.0	0.043	0.319	5.259	0.749	2.585	2.061	44	1.70
	III[1]	118.0	0.043	0.319	5.259	0.749	2.585	2.061	61	1.70
	IV[1]	160.0	0.043	0.319	5.259	0.749	2.585	2.061	45	1.70
	V[1]	150.0	0.085	0.500	3.333	0.469	1.670	2.366	76	1.70
	VI[1]	165.0	0.085	0.500	3.333	0.469	1.670	2.366	69	1.70
	VII[1,2]	354.0	0.043	0.340	4.854	0.396	1.583	2.650	33	2.05
	VIII[1]	336.9	0.043	0.355	4.698	0.391	1.556	2.834	72	1.80
500 kV	IX[2]	373.0	0.012	0.165	7.782	0.229	0.879	4.669	74	4.56
	X	157.0	0.019	0.276	6.869	0.414	1.331	3.434	56	1.54
	XI[1,2]	242.0	0.017	0.264	6.271	0.373	1.375	3.382	53	1.72
	XII[1,2]	385.35	0.016	0.256	6.243	0.320	1.322	2.860	44	1.62
	XIII[1]	201.0	0.017	0.265	6.237	0.355	1.419	3.742	64	1.53
	XIV[1]	201.0	0.017	0.268	6.206	0.251	0.980	3.491	64	1.53
	XV[1,2]	342.59	0.018	0.267	6.174	0.391	1.458	2.559	51	2.31
	XVI	333.0	0.017	0.303	5.660	0.242	1.011	3.396	58	1.96
	XVII[1,2]	385.4	0.025	0.313	5.217	0.311	1.230	3.584	59	1.67
	XVIII[1]	335.0	0.023	0.332	4.960	0.385	1.153	2.957	65	2.35
	XIX[1]	364.0	0.024	0.347	4.778	0.403	1.381	3.112	74	2.54
	XX[1,2]	242.0	0.024	0.347	4.778	0.403	1.381	3.112	66	1.91

[1]Double-circuit line. [2]Series compensated line.

With the presented analysis it is possible to observe how K' and R' varies with each line parameter and each shunt reactor parameter, which determines the suitability of the proposed SAED/SPAR method. Each parameter may define if the method is suitable or not. Now, according to the next section, it is possible to clearly indicate the suitability of the proposed secondary arc extinction method for any transmission line, based on the developed formulation.

D. Proposed SAED/ASPAR Application

A comparison between R, defined in (7) according to [28], and R' proposed in this paper and defined in (22), is shown in Table II for each line presented in Table I. For all the cases, R was greater than the threshold $\lambda = 1.28$, which erroneously indicate that the approach presented in [28] could be used for SAED/ASPAR with no constraints for all the analyzed lines. However, $R' < \lambda$ for Lines V, VI, IX, XVII, XVIII, XIX and XX, showing that this approach shall not be used for SAED/ASPAR in those lines. These findings are the basis for the proposed SAED/ASPAR methodology discussed in this paper.

The flowchart that summarizes the proposed methodology and its application to both non-compensated and shunt compensated lines is shown in Fig. 6. At first, it is necessary to define if the transmission line to be monitored is shunt compensated or not. If the line is not compensated, then the approach presented in [28] can be applied with no constraints. In addition, the proposed equations (21) and (22) could also be used. However, if the line is shunt compensated, only the proposed equations (21) and (22) can be used by acquiring the line and shunt compensation data (C_s, C_m, g and ρ), which are easily provided by power utilities. Finally, the obtained R' is compared to the threshold $\lambda = 1.28$. If $R' > \lambda$, then the approach for SAED/ASPAR can be safely applied for that SCTL. Conversely, if $R' \leq \lambda$, then the approach cannot be used for that line.

TABLE II
R AND R' FOR EACH LINE PRESENTED IN TABLE I.

Voltage	Line	R defined in (7) [28]	R' proposed in (22)
230 kV	I	2.55	4.75
	II	2.55	4.21
	III	2.55	11.79
	IV	2.55	4.32
	V	1.41	0.91
	VI	1.41	1.02
	VII	1.83	1.74
	VIII	1.66	1.38
500 kV	IX	1.67	0.59
	X	2.00	3.23
	XI	1.85	2.03
	XII	2.18	3.00
	XIII	1.67	1.98
	XIV	1.78	2.50
	XV	2.41	2.53
	XVI	1.67	1.38
	XVII	1.46	1.23
	XVIII	1.68	1.09
	XIX	1.54	0.72
	XX	1.54	1.11

IV. PROPOSED METHODOLOGY EVALUATION

The proposed methodology was evaluated by means of field oscillografic recordings from the Brazilian Power Grid. Therefore, typical transmission line phenomena were intrinsically taken into account here, including the Ferranti effect, reactive compensation, actual transposition scheme, secondary arc characteristics, measurements inaccuracies, double-circuit line coupling, etc. Although the proposed approach was explained assuming the lines to be fully transposed, its application to actual transposition schemes is proven here. Recordings of single-phase-to-ground faults followed by the faulty phase opening at different 230 and 500 kV SCTL were analyzed. For simplicity, the analysis was focused on Lines V, VII, and XI.

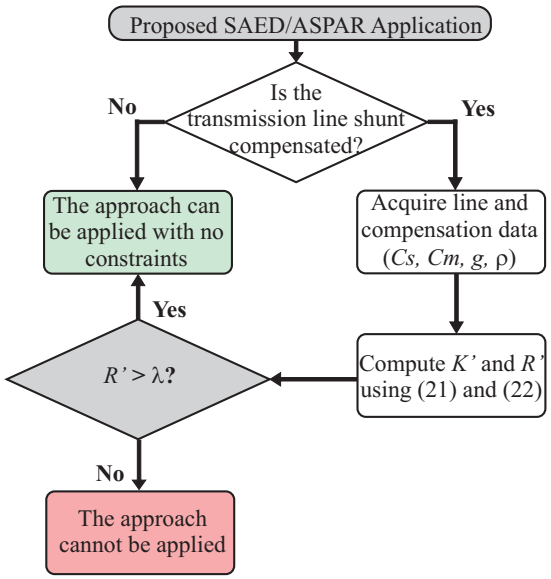

Fig. 6. Proposed Approach: Flowchart.

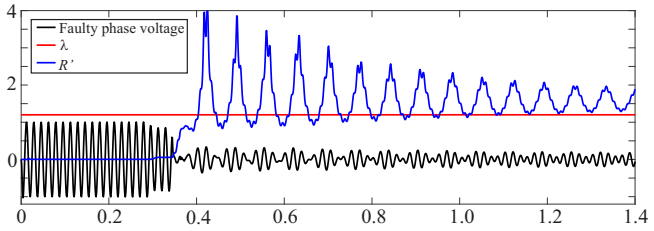

Fig. 7. Field recording of a single-phase to ground fault at the 230 kV Line VII and successful secondary arc extinction detection, as predicted by the proposed methodology.

According to Table II, the R' computed in agreement with (22) for the 230 kV Line VII was 1.74. Since 1.74 exceeds the threshold λ, it is concluded that the presented SAED/ASPAR approach can be safely applied to that line with no constraints. This is proven in Fig. 7 which shows the application of the presented SAED/ASPAR approach for a field recording of a single-phase to ground fault at Line VII. In that figure, the monitored line side faulty phase voltage is presented together with the threshold λ and the computed R'. The fault occurs around 0.3 s and then the faulty phase is opened around 0.36 s, establishing the secondary arc on the line. R' is close to 1 while the secondary arc persists. Then, around 0.4 s, R' increases higher than the threshold λ, successfully indicating that the actual temporary fault was quickly extincted and a recovery voltage is observed. The behavior of R' is according to the proposed formulation.

A similar analysis is accomplished for the 500 kV Line XI. In this case, according to Table II, the computed R' was 2.03, which exceeds the threshold λ. Thus, it is also concluded that the presented SAED/ASPAR approach can be safely applied to that line, as shown in Fig. 8 for a field recording of a single-phase to ground fault. In this case, the fault occurs around 0.5 s and the faulty phase is opened around 0.56 s. The secondary arc persists on the line until 1.12 s, which is

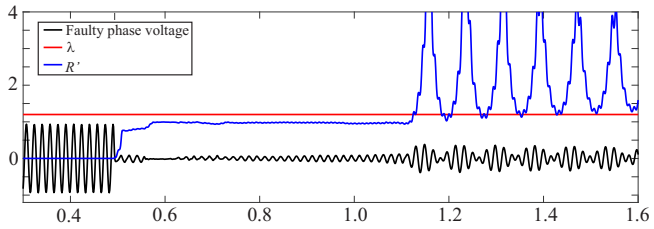

Fig. 8. Field recording of a single-phase to ground fault at the 500 kV Line XI and successful secondary arc extinction detection, as predicted by the proposed methodology.

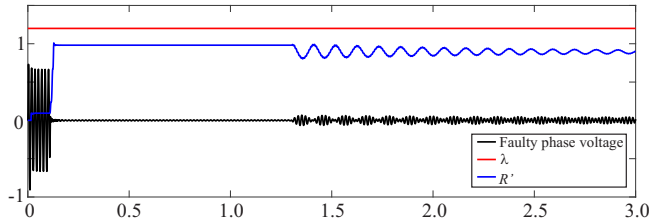

Fig. 9. Field recording of a single-phase to ground fault at the 230 kV Line V and unsuccessful secondary arc extinction detection, as predicted by the proposed methodology.

indicated by $R' \approx 1$. After that, R' increases higher than the threshold λ, signaling secondary arc extinction as predicted by the proposed methodology.

Finally, the application of the proposed methodology is evaluated for the 230 kV Line V. According to Table II, the computed R' for this line was 0.91. So, R' did not exceed the threshold λ, indicating that the presented SAED/ASPAR approach should not be applied to that line. This is due to the intrinsic characteristics of this line and its shunt reactors, causing R' to assume values close to 1 even after the arc extinction. In this case, it would not be possible to differentiate the arc extinction from its persistence in the line. Aiming to prove this condition, the presented SAED/ASPAR approach was applied for a field recording of a single-phase to ground fault at that line and the result is shown in Fig. 9, showing that R' remains below the threshold λ, despite the secondary arc extinction. In that figure, the faulty phase is opened around 0.1 s and the secondary arc persists until 1.3 s. However, even after its extinction, R' remains below the threshold λ, preventing the detection of arc extinction, as predicted by the proposed methodology.

V. Conclusions

In this paper, a new mathematical development has been proposed to extend the application of a practical and effective SAED/ASPAR approach to shunt-compensated transmission lines. The original approach, while effective for non-compensated lines, exhibited varying performance when applied to shunt-compensated lines, successfully detecting secondary arc extinction in some cases but failing in others. The proposed formulation addresses this limitation by incorporating the effects of shunt and neutral reactors, thereby enabling the method to reliably identify secondary arc extinction under a broader range of operating conditions.

Through the evaluation of field oscillographic recordings from the Brazilian Power Grid, the applicability of the proposed methodology was demonstrated for several 230 and 500 kV shunt-compensated transmission lines, accurately indicating the applicability of the presented approach, as for Line VII, or appropriately indicating the approach's limitations, as for Line V. These results confirm that the proposed methodology provides a robust framework for determining when this SAED/ASPAR approach can be safely applied, ensuring its practical utility for secondary arc extinction detection in shunt-compensated lines.

While the proposed methodology significantly improves the application of a practical phasor-based approach for secondary arc extinction detection in homogeneous shunt-compensated transmission lines, there are still cases where it fails to detect the arc extinction. These limitations shows the need for further developments aiming to adapt the presented approach to different operating conditions and make it universally applicable to any transmission lines configurations, including non-homogeneous lines, in which there are cable sections along the same transmission line.

REFERENCES

[1] K. M. C. Dantas, W. L. A. Neves, and D. Fernandes, "An approach for controlled reclosing of shunt-compensated transmission lines," *IEEE Transactions on Power Delivery*, vol. 29, no. 3, pp. 1203–1211, 2014.

[2] L. M. N. de Mattos, M. C. Tavares, and A. M. P. Mendes, "A new fault detection method for single-phase autoreclosing," *IEEE Transactions on Power Delivery*, vol. 33, no. 6, pp. 2874–2883, 2018.

[3] E. W. Kimbark, "Bibliography on single-pole switching," *IEEE Transactions on Power Apparatus and Systems*, vol. 94, no. 3, pp. 1072–1076, 1975.

[4] J. Esztergalyos, J. Andrichak, D. H. Colwell, D. C. Dawson, J. A. Jodice, T. J. Murray, K. K. Mustaphi, G. R. Nail, A. Politis, J. W. Pope, G. D. Rockefeller, G. P. Stranne, D. Tziouvaras, and E. O. Schweitzer, "Single phase tripping and auto reclosing of transmission lines-ieee committee report," *IEEE Transactions on Power Delivery*, vol. 7, no. 1, pp. 182–192, 1992.

[5] E. Godoy, A. Celaya, H. Altuve, N. Fischer, and A. Guzman, "Tutorial on single-pole tripping and reclosing," in *39th Annual Western Protective Relay Conference*, 2012.

[6] T. B. W. A. Khan and K. Jia, "A review of single phase adaptive auto-reclosing schemes for ehv transmission lines," *Prot Control Mod Power Syst*, vol. 18, no. 4, 2019.

[7] A. T. Johns and W. M. Ritchie, "Application of an improved technique for assessing the performance of single-pole reclosing schemes," *IEEE Transactions on Power Apparatus and Systems*, vol. PAS-103, no. 12, pp. 3651–3662, 1984.

[8] A. J. Fakheri, T. C. Shuter, J. M. Schneider, and C. H. Shih, "Single phase switching tests on the aep 765 kv system-extinction time for large secondary arc currents," *IEEE Transactions on Power Apparatus and Systems*, vol. PAS-102, no. 8, pp. 2775–2783, 1983.

[9] R. K. Aggarwal, A. T. Johns, Y. H. Song, R. W. Dunn, and D. S. Fitton, "Neural-network based adaptive single-pole autoreclosure technique for ehv transmission systems," *IEE Proceedings - Generation, Transmission and Distribution*, vol. 141, no. 2, pp. 155–160, 1994.

[10] S. P. Websper, A. T. Johns, R. K. Aggarwal, and R. W. Dunn, "An investigation into breaker reclosure strategy for adaptive single pole autoreclosing," *IEE Proceedings - Generation, Transmission and Distribution*, vol. 142, no. 6, pp. 601–607, 1995.

[11] M. Nagpal, S. Manuel, B. E. Bell, R. P. Barone, C. Henville, and D. Ghangass, "Field verification of secondary arc extinction logic," *IEEE Transactions on Power Delivery*, vol. 31, no. 4, pp. 1864–1872, 2016.

[12] C. Henville, H. A. Zhang, and M. Nagpal, "Field experience with enhanced hybrid single phase tripping and reclosing," in *Int. Conf. on Power Systems Transients (IPST), Seoul, South Korea*, 2017.

[13] X. Luo, C. Huang, Y. Jiang, and T. Tang, "Adaptive single-phase reclosure scheme for transmission lines with shunt reactors based on current inner product," *IET Generation, Transmission Distribution*, vol. 11, no. 7, pp. 1770–1776, 2017.

[14] S. Jamali and A. Ghaderi Baayeh, "Detection of secondary arc extinction for adaptive single phase auto-reclosing based on local voltage behaviour," *IET Generation, Transmission Distribution*, vol. 11, no. 4, pp. 952–958, 2017.

[15] F. Zhalefar, M. R. Dadash Zadeh, and T. S. Sidhu, "A high-speed adaptive single-phase reclosing technique based on local voltage phasors," *IEEE Transactions on Power Delivery*, vol. 32, no. 3, pp. 1203–1211, 2017.

[16] I. Nikoofekr and J. Sadeh, "Determining secondary arc extinction time for single-pole auto-reclosing based on harmonic signatures," *Electric Power Systems Research*, vol. 163, pp. 211 – 225, 2018.

[17] N. Jiaxing, H. Baina, W. Zhenzhen, and K. Jie, "Algorithm for adaptive single-phase reclosure on shunt-reactor compensated extra high voltage transmission lines considering beat frequency oscillation," *IET Generation, Transmission Distribution*, vol. 12, no. 13, pp. 3193–3200, 2018.

[18] O. Dias, M. C. Tavares, and F. Magrin, "Hardware implementation and performance evaluation of the fast adaptive single-phase auto reclosing algorithm," *Electric Power Systems Research*, vol. 168, pp. 169 – 183, 2019.

[19] X. Xie and C. Huang, "A novel adaptive auto-reclosing scheme for transmission lines with shunt reactors," *Electric Power Systems Research*, vol. 171, pp. 47 – 53, 2019.

[20] S.-A. Ahmadi, M. Sanaye-Pasand, P. Jafarian, and H. Mehrjerdi, "Adaptive single-phase auto-reclosing approach for shunt compensated transmission lines," *IEEE Transactions on Power Delivery*, vol. 36, no. 3, pp. 1360–1369, 2021.

[21] A. Ghaderi Baayeh and S. Jamali, "Optimal auto-reclosing time for shunt compensated transmission lines using synchrosqueezing wavelet transform," *International Journal of Electrical Power & Energy Systems*, vol. 128, p. 106744, 2021. [Online]. Available: https://www.sciencedirect.com/science/article/pii/S0142061520342897

[22] M. Saad, N. Munir, and C.-H. Kim, "Pattern recognition based auto-reclosing scheme using bi-directional long short-term memory network," *IEEE Access*, vol. 10, pp. 119 734–119 744, 2022.

[23] M. Saad, C.-H. Kim, and N. Munir, "Single-phase auto-reclosing scheme using particle filter and convolutional neural network," *IEEE Transactions on Power Delivery*, vol. 37, no. 6, pp. 4775–4785, 2022.

[24] F. Gatta, A. Geri, M. Graziani, S. Lauria, and M. Maccioni, "Single-pole autoreclosure in uncompensated ehv ac mixed overhead-cable lines: A parametric time-domain analysis," *Electric Power Systems Research*, vol. 210, p. 108055, 2022. [Online]. Available: https://www.sciencedirect.com/science/article/pii/S0378779622002802

[25] X. Xie, Z. Huang, X. Fan, and T. Tang, "Adaptive single-phase auto-reclosing scheme based on the moving average filter-quadrature signal generator for transmission lines with shunt reactors," *Electric Power Systems Research*, vol. 223, p. 109545, 2023. [Online]. Available: https://www.sciencedirect.com/science/article/pii/S0378779623004340

[26] N. Tong, J. Li, G. Li, W. Huang, R. Cao, and Y. Wang, "Soft single-pole reclosing control for mmc-connected ac transmission lines," *IEEE Transactions on Power Delivery*, vol. 39, no. 5, pp. 2841–2854, 2024.

[27] K. Dantas, F. Lopes, K. Silva, F. Costa, N. Ribeiro, and L. Gama, "Leveraging existing relays to improve single phase auto-reclosing," *Electric Power Systems Research*, vol. 212, p. 108457, 2022. [Online]. Available: https://www.sciencedirect.com/science/article/pii/S0378779622005727

[28] K. M. C. Dantas, F. V. Lopes, K. M. Silva, F. B. Costa, and N. S. Ribeiro, "Phasor-based single-phase auto-reclosing scheme for non-compensated transmission lines," *IEEE Transactions on Power Delivery*, vol. 37, no. 1, pp. 219–229, 2022.